

Chemically-reacting, transverse plume

P. Ranjan, K. Perez, T. Alvarado, B. Potter*, & R. E. Breidenthal

University of Washington

*William E. Boeing Department of Aeronautics and Astronautics
Box 352400 Seattle, WA 98195-2400 USA*

breident@aa.washington.edu

*Pacific Wildland Fire Sciences Laboratory, USDA Forest Service
(Received ; published)

The flame length of a plume in incompressible cross-flow is analyzed and the results are compared with those obtained in a reacting water tunnel experiment. It is argued that the axial vortex pair in the flow arises from the plume momentum normal to the free stream, the momentum flux being equivalent to the impulse from the buoyant force.

DOI:

PACS Number(s): 47.70.Fw,47.70.Pq,47.51.+a

I. INTRODUCTION

The structure, trajectory and mixing rate of transverse jets have been investigated in numerous experiments, such as in [1-5]. The jets are driven by the initial momentum flux from the nozzle, without buoyancy differences between the jet fluid and the ambient fluid. A prominent feature of the flow is a pair of counter-rotating vortices. In the far field, those vortices are nearly parallel and move with the freestream. [6] (henceforth BB) argue that a temporal, two-dimensional vortex pair can model the dynamics and mixing, resulting from a line impulse. Above the mixing transition, the mixing is entrainment-limited; so that BB's simple dilution model [6] describes the mixing rate, to within an adjustable constant. It appears that the buoyancy-driven plume has been less studied [7-8]. In contrast to the jet, the conserved quantity for such a plume is the buoyancy force rather than the jet thrust. [9] presented an analysis of a source of buoyancy and [10] extended this to allow for mass, momentum and buoyancy. As described in detail in the sections to follow, [10] determined the location of the mixing transition for a plume without cross-flow and considered the case of momentum being in the vertical direction and of the same sign as the buoyancy forces. Other authors such as [11] and [12] presented numerical schemes for evaluating forced and angled plumes with a given set of initial conditions. [13] proposed a mathematical model that clearly presented a division of vertical plumes into three basic categories: buoyant jets,

mass sources, and pure plumes. The main focus of their work was however concentrated on studies of angled plumes. The mathematical model presented by [13] is found to be valid only for cases with buoyancy and momentum flux with the same sign.

II. ANALYSIS

The present paper is a direct application of the ideas developed for transverse jet by BB to transverse plumes. The appropriate temporal problem for the transverse jet is the line, or two-dimensional, vortex pair. For the transverse plume, the temporal problem is the two-dimensional thermal. The temporal problem should be a valid approximation of the corresponding spatial problem if the curvature of the spatial flow can be ignored. This approximation is expected to be asymptotically valid in the far field of the flow, where the curvature asymptotically vanishes.

The conserved quantity is the buoyant force per unit length and per unit mass

$$B = \text{const.} \frac{g'_0 V_n A_0}{V_\infty} = \frac{\text{length}^3}{\text{time}^2}, \quad (1)$$

where g' is the buoyancy acceleration. The subscript "0" indicates the initial value at the nozzle. The nozzle velocity is V_n , the nozzle area is A_0 , and the freestream velocity is V_∞ .

From dimensional considerations

$$\delta(t) = \text{const.} B^{1/3} t^{2/3}, \quad (2)$$

where $\tilde{\delta}(t)$ is the vortex size as a function of time t .

Assuming a Galilean transformation, the downstream station x is related to t by

$$x = V_\infty t, \quad (3)$$

and the spatial problem becomes

$$\frac{\delta(x)}{l} = \text{const.} \left(\frac{x}{l}\right)^{2/3} \quad (4)$$

Where

$$l \equiv \frac{B}{V_\infty^2} \quad (5)$$

is an intrinsic length scale of the problem.

Eq. (4) for the transverse plume contrasts with

$$\frac{\delta}{l_j} = \text{const.} \left(\frac{x}{l_j}\right)^{1/3} \quad (6)$$

for the transverse jet, where the corresponding length scale is

$$l_j = \left(\frac{T}{\rho V_\infty^2}\right)^{1/2} \quad (7)$$

according to [6]. Here T is the jet thrust and ρ is the freestream density.

III. MIXING AND FLAME LENGTH

The flame length is derived using Broadwell's dilution argument in BB. Per unit time, the volume of mixed fluid at the flame tip divided by the volume of nozzle fluid must be proportional to $(\phi + 1)$, where ϕ is the volume equivalence ratio of ambient to nozzle fluid necessary to react all the nozzle fluid. So

$$\frac{V_\infty \delta_f^2}{V_n A_0} = \text{const.} (\phi + 1) \quad (8)$$

where δ_f is the vortex size at the flame tip.

Eq. (1)-(8) yield

$$\frac{x_f}{d} = \text{const.} \left(\frac{V_n^2}{g_0 d}\right)^{1/2} \left(\frac{V_\infty}{V_n}\right)^{3/4} (\phi + 1)^{3/4}, \quad (9)$$

where x_f is the streamwise station at the flame tip and d is the nozzle diameter. The flame length depends weakly on the nozzle Richardson number,

$$Ri_0 \equiv \frac{g_0 d}{V_n^2}. \quad (10)$$

We have implicitly assumed that the nozzle thrust is sufficiently small compared to the buoyant flux. This assumption is not true at the nozzle if Ri_0 is less than one. Further from the nozzle, however, the accumulated impulse of a continuous buoyant force eventually surpasses that of a jet, so that Eq. (9) should be asymptotically valid at sufficiently large equivalence ratio. [10] determined the location of this transition for a plume without cross-flow.

With a cross-flow, the transition between a momentum-dominated flow and a buoyancy-dominated flow can be estimated by equating the impulse per unit length of the jet with the plume in their corresponding temporal problems.

They are equal at time

$$t^* = \frac{T/\rho}{BV_\infty}, \quad (11)$$

corresponding to station

$$x^* = \frac{T/\rho}{B}. \quad (12)$$

This can be expressed as

$$x^* = \frac{\rho_0 V_\infty V_n}{\rho g_0}, \quad (13)$$

where ρ_0 is the density of the injected fluid. Eq. (10) is expected to be valid if $x^* \ll x_f$.

IV. EXPERIMENT

An aqueous plume was introduced through the test-section ceiling of a water tunnel, which provided the cross-flow (Fig 1 and Fig 2). The water tunnel apparatus is described in [14]. Briefly, the test section is 0.7 m high x 0.7 m span x 3 m long, through which a dilute and transparent solution of sulfuric acid flowed. A red solution of sodium hydroxide, sodium chloride, and phenolphthalein (a pH indicator) drained into the water tunnel through a jet nozzle of 0.019 m diameter from a reservoir above the water tunnel. The solution drained exclusively under gravitational flow, with no other momentum source. When the two fluids mixed, a rapid chemical reaction caused the red injected solution to disappear. The volume equivalence ratio (the volume ratio of ambient to inject fluid

required to effect dilution and disappearance) was varied by changing the relative concentrations of the acid and base. The velocity of the jet was estimated from the measured volume flow rate as determined by the rate at which liquid emptied from the reservoir. No correction was made to the velocity profile for the thickness of the nozzle boundary layer

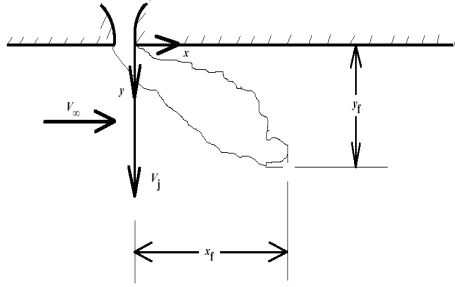


FIG. 1. Flow geometry

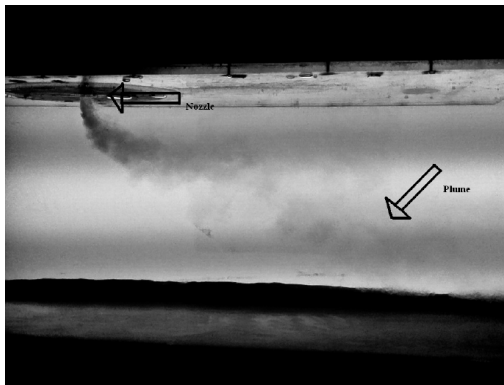


FIG. 2. Flow visualization at $U_f=0.11 \text{ m s}^{-1}$, $V_n=0.12 \text{ m s}^{-1}$ 20.66, $x_f = 0.9 \text{ m}$, $Re_f = 10,000$.

The nozzle Reynolds numbers Re_o varied between 400 and 6000. While this range is not always above the Reynolds number of the mixing transition, approximately a few thousand, the important requirement for the flame length is that the mixing be entrainment-limited by the flame tip. So the Reynolds number at the flame tip must be sufficiently large. From Eq. (2) through (10), it is

$$Re_f \cong \left(\frac{g'_0 V_n A_0}{V_\infty} \right)^{2/3} \left(\frac{x_f}{V_\infty} \right)^{1/3} \frac{1}{\nu}, \quad (15)$$

where ν is the kinematic viscosity of the fluid. The Reynolds number at the flame tip varied from 1000 to 21,000.

The coordinates at the end of the red flame were estimated visually. This measurement was performed using video recording technique with the help of a 6.1 mega-pixel camera with 3X optical zoom (35 mm equivalent: 36–108 mm) which permitted taking pictures with a shutter speed of 1/1400 sec, providing an appropriate resolution of the flame end.

The nozzle fluid was nearly saturated with salt in order to minimize the fraction of the total flame length that was influenced by jet speed rather than buoyancy. The tunnel speed was progressively varied, so that the velocity ratio of freestream to nozzle flows varied from 0.6 to 22.

The chord flame length is defined in terms of the flame tip coordinates.

$$c_f \equiv (x_f^2 + y_f^2)^{1/2}. \quad (16)$$

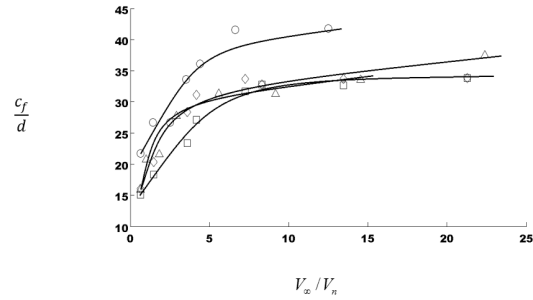


FIG. 3. Chord length of the “flame” for various values of equivalence ratio: 22.4(O); 21.32 (□); 20.7 (Δ); 18.3 (◇).

It is plotted as a function of the velocity ratio for different values of equivalence ratio in Fig 3. Finally, the streamwise flame length is shown in Fig 4, and in normalized form in Fig 5. While there is considerable scatter, the results are in accord with the model, which predicts a constant value of the normalized flame length for all velocity ratios. The dimensionless flame length X_f is expressed as

$$X_f = \frac{x_f}{d \left(\frac{V_n}{g'_0 d} \right)^{1/2} \left(\frac{V_\infty}{V_n} \right)^{3/4} (\phi+1)^{3/4}}. \quad (17)$$

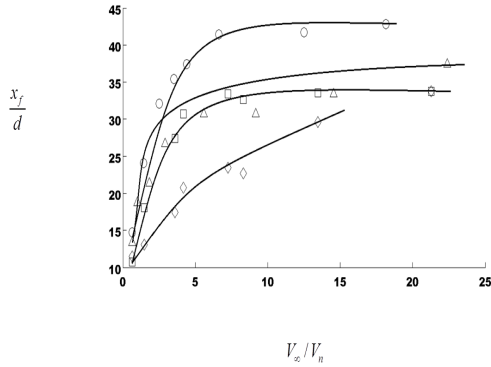


FIG.4. Downstream flame length for various values of equivalence ratio 22.4(O); 21.32 (□); 20.7 (Δ); 18.3 (◇).

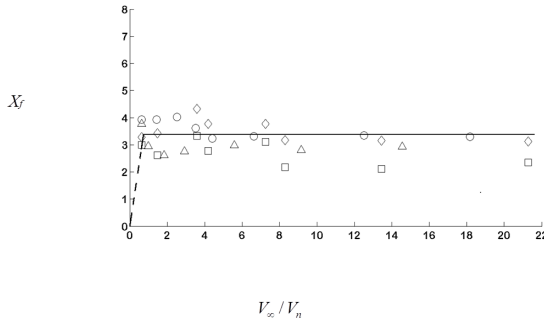


FIG.5. Normalized downstream flame length. Notation as in FIG. 3.

V. DISCUSSION

As with the transverse jet, the flame length of the transverse plume is independent of the Reynolds number Re_0 above the mixing transition [6]. All data shown are from this regime. For lower Reynolds numbers, the flame length is much longer in an aqueous flow. This behavior, typical of mixing in turbulent flows, is due to the sensitivity of the mixing rate to the presence of small-scale turbulent motions. The critical value for this mixing transition is of the order of a thousand.

According to Eq. (9), the model predicts that the streamwise flame length x_f/d should vanish in the limit of $V_\infty/V_n \rightarrow 0$. Furthermore, the flame

length goes as $(\phi+1)$ raised to the 3/4 power. However, it is clear that the chord flame length

c_f/d cannot vanish in that limit. Furthermore, similarity requires that the flame length be proportional to $(\phi+1)$ there. Experiments by [15], [16], [17] and others all show that the buoyant fluid must travel a specific distance from its source in order to entrain and to mix sufficient ambient fluid to dilute the source fluid to a specified concentration. As a consequence, the chord flame length at any equivalence ratio is finite for $V_\infty/V_n = 0$. It is clear that two different regimes exist, with a transition between them at some $V_\infty/V_n > 0$, where the chord flame length is a minimum.

From Fig 3, the velocity ratio for minimum chord flame length is evidently less than about 0.6. This is consistent with the value of about 0.06 observed in the transverse jet, [6]. Such a minimum is expected to correspond in both flows to the formation of a pair of counter-rotating vortices. At this transition, the chordwise flame length is a minimum, corresponding to the most rapid entrainment. In the case of a fire, this would be the most intense fire.

VI. APPLICATION TO WILDFIRES

This study was originally motivated by questions related to wildland fire behavior. Among other factors, wildland fires are influenced by the intensity (energy release rate) of the fire, the rate of spread, and the variability of these properties over time. An intense, fast moving fire with highly variable rate or direction of spread is dangerous for fire fighters and more difficult to bring under control. Any insight into the properties likely to produce particularly dangerous fire behavior has the potential to save lives, as well as thousands of dollars.

When applied to a wildland fire, it is first important to distinguish what is meant by flame length. The term “flame” as used previously in this paper refers to the visible mixing portion of the buoyant outflow where combustion is occurring.

In the wildland fire context, the minimum flame length mentioned previously corresponds to the maximum mixing, which would lead to the most turbulent fire behavior. The integrated buoyancy flux F over the fire area is

$$F \equiv \frac{gE}{\rho c_p \Theta}, \quad (18)$$

with dimensions $\text{length}^4/\text{time}^3$. A simple dimensional argument suggests that the most intense fire would occur for a critical wind speed

$$V_{\infty crit} \cong F^{1/3} D^{-1/3} = \left(\frac{gE}{\rho c_p \Theta D} \right)^{1/3}, \quad (19)$$

where D is some measure of the transverse width of the fire at the surface. Using h to indicate the heat content of the fuel (J kg^{-1}), w to indicate the areal fuel density (kg m^{-2}) and r to indicate the fire's rate of spread (m s^{-1}) this can be written as

$$V_{\infty crit} = \left(\frac{ghwr}{\rho c_p \Theta} \right)^{1/3}. \quad (20)$$

Because the water tunnel design approximates a ‘‘point source’’ fire, it is most relevant to a fire where the transverse and longitudinal extents are comparable, or small. As an example application of this, consider the 2003 Canberra fire in Australia. The estimated fuel load and rate of spread for this fire are 2.5 kg m^{-2} and 1.3 m s^{-1} , respectively. The heat content of forest fuels is approximately 17 MJ kg^{-1} . Using these fire properties with appropriate values for g , ρ , c_p , and Θ (9.8 m s^{-2} , 1.1 kg m^{-3} , $1004 \text{ J kg}^{-1} \text{ K}^{-1}$ and 300 K , respectively) then yields a critical wind speed of 12 m s^{-1} , or 43 km h^{-1} . This suggests that eq (20) may provide reasonable wind speed values, given real values for the input parameters.

The flame length of a real fire would be slightly different from that in the water tunnel. In the water tunnel, the flow has all of the buoyancy introduced at the nozzle. In a real fire, on the other hand, buoyancy is continuously added from the origin to the flame tip.

Another flow feature that may threaten firefighters is Fric & Roshko lee vortices [18], shown in Fig 6. While these tornado-like

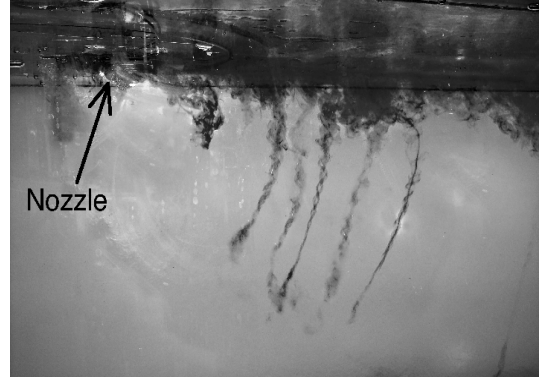


Fig 6. Flow visualization of the Fric & Roshko vortices. The nozzle is in the upper left corner.

vortices seem to have little effect on the far-field flame length of the plume, they may play a critical role in some wildland fires by first lofting and then propagating burning embers downwind, as noted by [19]. Firebrands sometimes overrun and defeat fire breaks constructed by firefighters, igniting new fires downwind of old ones.

VII. CONCLUDING REMARKS

The analysis and the comparison of the results with observation have concentrated on the far-field behavior of transverse plumes. From the conservation of buoyant force, the growth law of the corresponding temporal flow has been derived. A simple dilution argument then predicts the flame length of the spatial flow. The measured flame length of the transverse plume is in reasonable agreement with this description of the far-field behavior. Notably, there is a minimum in the flame length at an intermediate velocity ratio. This suggests the approximate conditions for the most intense wildfires.

ACKNOWLEDGMENTS

The second and third authors are pleased to acknowledge support from the HACU Internship program.

- [1] J. KEFFER and W.D. BAINES, *J. Fluid Mech.* **15**, 481 (1962).
- [2] Y. KAMOTANI and I. GREBER, *AIAA J.* **10**, 1425 (1972).
- [3] S.H. SMITH and M.G. MUNGAL, *Fluid Mech.* **357**, 83 (1998).
- [4] L. CORTELEZZI and A.R. KARAGOZIAN, *J. Fluid Mech.* **446**, 347 (2001).
- [5] A. R. KARAGOZIAN, *Progress in Energy and Combustion Science*, **36**(5), 531 (2010).
- [6] J.E. BROADWELL, and R.E. BREIDENTHAL, *J. Fluid Mech.* **148**, 405 (1984).
- [7] J.H. MIDDLETON, *Boundary Layer Meteorol.* **36**, 187 (1986).
- [8] M.W. GOLAY, *Atmos. Environ.* **16**, 2373 (1982).
- [9] B.R. MORTON, G.I. TAYLOR and J.S. TURNER, *Proc. R. Soc.* **234**, 1 (1956).
- [10] B.R. MORTON, *J. Fluid Mech.* **2**, 151 (1959).
- [11] K. HOFER, and K. HUTTER, *J. Non-Equil Thermodyn.* **6**, 31 (1981).
- [12] M. SCHATZMANN, *J. Appl. Math. Phys. (ZAMP)* **29**, 608 (1978),
- [13] G.F. LANE-SERFF and P.G. BAINES, *J. Fluid Mech.* **363**, 229 (1998).
- [14] A. EROGLU and R.E. BREIDENTHAL, *AIAA J.* **36**(6), 1003 (1998).
- [15] J. ROUSE, C.S. Yih, and J.W. HUMPHREY, *Tellus* **4**, 201 (1952).
- [16] P.N. PAPANICOLAOU, and E.J. LIST, *Intl. J. Heat Mass Transfer*, **30**, 2059 (1987).
- [17] A. SHABBIR and W.K. GEORGE, *J. Fluid Mech.* **275**, 1 (1994).
- [18] T.F. FRIC and A. ROSHKO, *J. Fluid Mech.* **279**, 1 (1994).
- [19] P. CUNNINGHAM, S.L. GOODRICK, M.Y. HUSSAINI, and LINN, *Int. J. Wildland Fire* **14**, 61 (2005).